



# Experimental Evaluation of Slenderness Ratio of Composite Column Reinforced by Multi-skin Steel Tubes

Nagham M. Salim<sup>1</sup> · Alaa M. Al-Khekany<sup>1</sup>

Received: 26 December 2020 / Accepted: 9 June 2021 / Published online: 21 June 2021  
© King Fahd University of Petroleum & Minerals 2021

## Abstract

Concrete-filled steel tube (CFST) is a composite section which has more ultimate strength than concrete or steel section alone. This experimental study was conducted to estimate the slenderness ratio of composite concrete-filled multi-steel tubes (CFMST) columns. In this study, 55 composite columns with various heights were fabricated and tested under axial load. They were divided into two main groups depending on the shape of the cross section (circular and square cross section). Both sections have the same external dimensions. Each group includes five subgroups; solid and hollow columns with various numbers of steel layers of different heights. The mode of column failure was used to categorize the columns into non-slender (short) or slender (long) columns. The experimental results exhibited two types of failure modes: local buckling for non-slender columns and global buckling for slender columns. The slenderness ratio ( $\lambda$ ) of all samples was calculated mathematically whereby the suggested equation is dependent on the cross-section geometry to specify the slenderness limit of CFST with various numbers of steel tubes. The results show the new proposed equations can be used to predict the slenderness limit of CFST with various numbers of steel tubes, and thus whether the column will behave as slender or non-slender. The results showed that the CFMST with solid section and multiple skins has higher slenderness limit where it increased from (26.12 to 66.12) mm and (53.62 to 129.4) mm for circular and square section for one to three layers, respectively. The proposed equations of slenderness ratio of CFST depend on the ratio of steel area to concrete area in composite cross section. Also, the ultimate strength of the composite section is increased with the increase in the number of skins due to increased confinement of concrete.

**Keywords** Composite column · Double skins · Multi-skins · Slenderness ratio · Steel tube

## 1 Introduction

Concrete-filled multi-skin steel tube (CFMST) columns are an engineered structure of composite members, [1] consisting of two or more (circular, square, or rectangular) steel tubes. CFMST columns are good-performance structural elements that have been widely used in tall and multi-story building structures. There is no need to use formwork for this type of member where the column is the formwork. This leads to reductions in working time, which is an important advantage when using this type of column. Concrete-filled steel tube (CFMST) columns have high strength due to the strength of their materials (concrete and steel), which

makes them more economical. Because CFMST reduces the required cross-section size of the column, it allows more space when constructing structures. CFMST columns have a high resistance to fire as the sandwiched-concrete dictates the steel tube and protects it from high temperatures better than composite column with one layer of steel tube (CFST). However, because of the presence of the internal pipe, the concrete infill should be designed to be more flowable and have a high passing ability. This problem can be resolved by combining cementitious fillers or inert fillers inside the concrete as explained by Lai et al. [2, 3]. Tests on the structural performance of concrete-filled double skin steel tubular (CFDST) columns with axial loading have been performed by previous researchers [4–11].

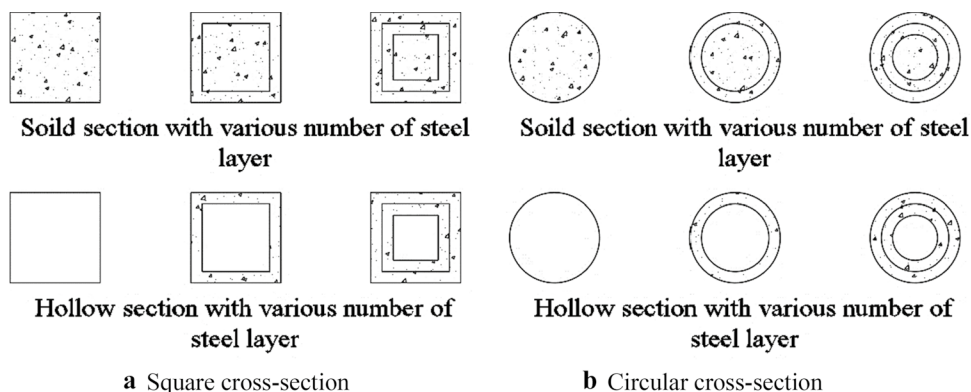
The steel tubes are placed vertically and their annuals space is infilled by concrete infill [12]. Figure 1 depicts the cross-sectional details of the concrete-filled steel tube (CFST) column [13]. The basic principle holding in the

✉ Alaa M. Al-Khekany  
Alaa.Alkhekany@qu.edu.iq

<sup>1</sup> Civil Engineering Department, University of Al-Qadisiyah, Ad Diwaniyah, Iraq



**Fig. 1** Types of CFST column [13]



composite columns is that steel pipes work as formwork as well as main and lateral reinforcing steel. The samples are partly or entirely loaded, the concrete core constrains the local buckling of the pipes and thus, the pipes constrict the concrete, causing the concrete to advance the load resistance. Major features of concrete-filled steel tube CFST columns are: construction is simple, formwork is not needed, light weight with increased steel resistance make it suitable for use on small and light foundations [12]. Steel tubes forming the column provide better conditions for curing the concrete, increasing its strength [14]. Their use in multi-story buildings and piers is recommended owing to the benefit of increased load capacity for a reduced cross section [15]. Concrete-filled steel tube (CFST) columns are studied and widely applied in civil and structural engineering [16].

In CFST columns, the concrete and steel together resist exterior loads by combining behavior due to bond and friction between steel tube and concrete. Supplementary strut in the concrete casing prevents undue spalling of the concrete under conditions of uniform loading. In a composite structure, the steel tube section carries the initial construction loads, including structural weight during construction. After that, the concrete is pumped into the steel pipes. The concrete and steel are combined in such a way that the advantages of the materials are effectively used in the composite column. The subsequent addition of concrete to the building frame allows for reduced impact and lateral deflection [17].

There have been experimental investigations on concrete-filled steel tubes CFST over many decades [18]. Several previous studies were conducted to identify the structural behavior of the concrete-filled tube columns CFST in the round section, such as Xiong et al. [10], Furlong [19], Knowles and Park [20], Neogi et al. [21], Rangan and Joyce [22], Zeghiche and Chaoui [23], Portolés et al. [24], Dundu [25] Ekmekyapar and Al-Eliwi [26]. Ekmekyapar and Al-Eliwi experimental results [26] proved that increasing of slenderness of the column reduced the confinement of the concrete core in round CFST columns. This was because the primary indicator of the ultimate strength

of the slender column is global buckling failure, not the strength of the material, as the strength of the concrete is impacted by the property of confinement. Moreover, Tao et al. [27] studied the behavior of structural double-skin (DCFST) slender columns under eccentrically loading as shown in Fig. 1b. All specimens of slender DCFST columns had a failure pattern of buckling. It was confirmed that the bending rigidity and the ultimate capacity of the samples studied were reduced, due to an increase in the eccentric loading or an increase in the slenderness ratio of the column.

Romero et al. [28] presented a case study on the behavior of slender round concrete-filled double skin steel tube CFDST columns exposed to room and high temperatures. The main parameters studied in this research were the thickness of the steel layer and various concrete strengths on the inner and outer steel tubes. The results showed the effect of steel tube thickness on column strength, namely that an increase in the thickness of the outside tube combined with a thinner internal tube led to a good improvement in the ultimate of CFDST slender columns. Ibanez et al. [9] examined slender round CFDST beam-columns under eccentricity loading, where the members had relative strength ratios between 0.53 and 1.17. Several concrete compressive strengths were used to create these slender beam-columns; these ranged between 40 and 149 MPa. All the slender CFDST columns failed by global buckling. Wan and Zha [29] introduced verification in the behavior of round slender and non-slender CFDST columns under the influence of eccentric loading to failure. It turned out that the strength of non-slender columns is improved when using an inner tube with a larger diameter, whereas in slender columns this effect is less clear. Recently, Ahmed et al. [11] presented experimental results on non-slender round CFDST columns examining the sensitivity of their structural performance to the eccentric load, the cross-sectional shape, and the thickness of steel tube. Experimental data from similar research [30] showed that the internal tube considerably enhanced the flexibility of CFDST columns and the stiffness and strength



reduced significantly with increases in the eccentricity ratio with increasing the eccentricity ratio remarkably.

From the above previous studies, it found that there do not try by these researchers to propose an equation to estimate the slenderness ratio for CFMST composite column. Hence, the main aim of this study is to estimate the limit of the slenderness ratio for CFST columns. However, no computational model has been developed to investigate their slenderness ratio and no design guidelines have been given in the predicted slenderness ratio of such columns. To overcome these limitations, this paper describes new suggested equations to calculate the slenderness ratio of CFST columns reinforced with various numbers of steel tube skins filled with normal concrete, this has not often been calculated by other researchers. The verifications of the suggested equations are

undertaken depending on the adopted experimental study. The determination of the column type whether non-slender (short) or slender (long) was obtained experimentally depending on the failure mode of the tested samples.

## 2 Experimental Program

In this work, HSS steel tubes were used to fabricate the adopted samples. The samples were of circular and square cross section, with heights ranging from (400 to 800) mm in the circular sections and (800 to 1200) mm in the square sections. Total samples were (55) tested under axial load as shown in Table 1.

**Table 1** Adopted column specimens

Core type of column	Circular section			Square section			
	Label of specimens	Height of column (mm)	Specimen designation	Label of specimens	Height of column (mm)	Specimen designation	
Solid section	C1S	450	C1S450	S1S	800	S1S800	
		500	C1S500		850	S1S850	
		550	C1S550		900	S1S900	
		600	C1S600		950	S1S950	
		650	C1S650		1000	S1S1000	
		700	C1S700		1100	S1S1100	
	C2S	500	C2S500	S2S	800	S2S800	
		550	C2S550		850	S2S850	
		650	C2S650		900	S2S900	
		700	C2S700		950	S2S950	
		750	C2S750		1000	S2S1000	
		–	–		1100	S2S1100	
	C3S	500	C3S500	S3S	1000	S3S1000	
		550	C3S550		1050	S3S1050	
		600	C3S600		1100	S3S1100	
		650	C3S650		1150	S3S1150	
		700	C3S700		1200	S3S1200	
		750	C3S750		–	–	
	Hollow section	C2H	400	C2H400	S2H	700	S2H700
			450	C2H450		750	S2H750
			500	C2H500		800	S2H800
550			C2H550	850		S2H850	
600			C2H600	900		S2H900	
–			–	–		–	
C3H		500	C3H500	S3H	900	S3H900	
		550	C3H550		950	S3H950	
		600	C3H600		1000	S3H1000	
		650	C3H650		1050	S3H1050	
		700	C3H700		1100	S3H1100	
		–	–		–	–	
		–	–		–	–	
		–	–		–	–	
Total no. of specimens	28 specimens			27 specimens			

## 2.1 Preparation of Specimens

A total of (55) samples were fabricated and filled with normal strength concrete (NSC) as shown in Table 1 and Fig. 2. NSC mix proportions of (1:1.6:2.94) (Cement: Sand: Gravel) proportions, respectively, with W/C ratio of (0.45) was designed based on ACI code (ACI 211.1-1991) [31] and utilized to cast the columns. The compressive strength ( $f'_c$ ) of this mixture at 28 days was (32.2 MPa). Each specimen was prepared a steel tube of a specific height, and the number of steel layers depended on the adopted sample. A base steel plate was used to close the bottom end of the column while the other end was open to allow infilling with NSC. The specimens in Table 1 were categorized according to the cross section of CFST as either circular section or square section. Each category was divided into five groups depending on the core type of column and the number of steel tubes. The number of steel tube layers varied from one to three with various heights of columns. The height for circular sections varied/ranged from (400–800) mm and for a square section from (700–1200) mm. The design of columns was based on determination of the critical height of these columns that represent the limit in the CFMST column can be classified as short or long column. Many parameters were adopted in this study; shape of cross section (square or circular section), number of steel layers, section type (hollow or solid section). All these parameters play a role in the determination of the critical height. Therefore, for multilayer specimen (for example C2S), the lower bond of the height

was higher than the section with only one layer (C1S). The reason behind that is as the inertia of the section increased, the critical height increased and so on for other parameters. These specimens were adopted to predict the slenderness ratio of CFST with various parameters. All steel tubes in the adopted specimens have the same thickness (1 mm). The specimen designations in Table 1 are as follows: the first symbol (C or S) refers to the cross section, i.e., (C) for circular section and (S) for square section; the second symbol (1, 2 or 3) refers to the number of layers of steel tube for the specimen; the third symbol (S or H) indicates whether the core of the specimens is solid or hollow; the final number refers to the height of the specimen in millimeters. In all specimens, circular and square specimens have the same external dimension as shown in Fig. 3, i.e., the width of the square column ( $W$ ) equals the diameter of the circular tube ( $D$ ) = 76.2 mm.

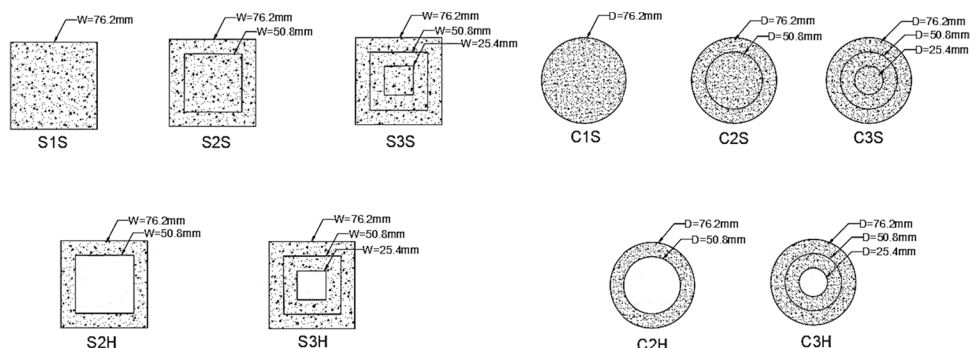
## 2.2 Testing Procedure

All samples were tested under axial load by using a universal testing machine with 2000 kN maximum capacity. The specimen was installed vertically and supported at the free ends by bases of steel plate of the testing machine as shown in the schematic diagram plan of the testing procedure (Fig. 4). Two Linear Variable Displacement Transducers (LVDTs) were used for lateral displacement measurement. LVDT1 and LVDT2 with ( $90^\circ$ ) between them were placed at mid-height of the tested specimen to measure the lateral

**Fig. 2** Fabrication and casting of specimens



**Fig. 3** Cross section and details of the adopted specimens



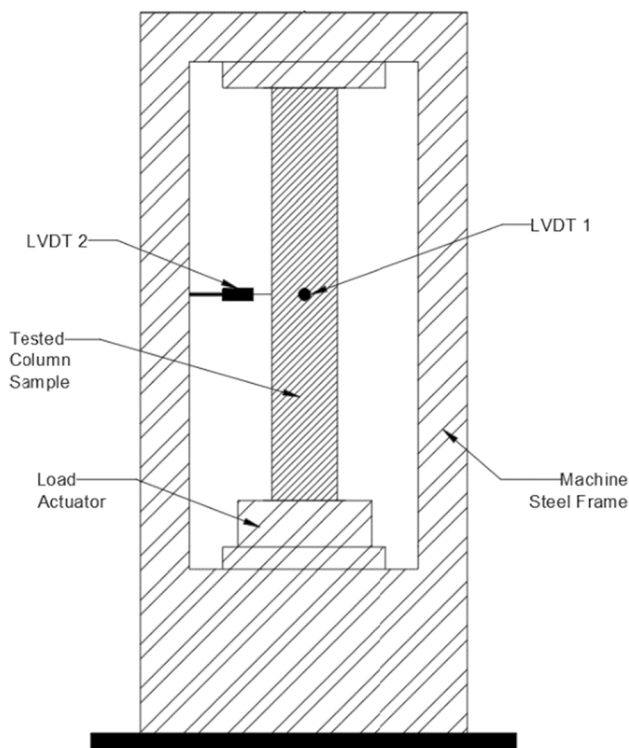


Fig. 4 Set up of the testing procedure

displacement (buckling) of the tested sample on both sides of the specimen due to applied axial load as shown in Fig. 4.

### 3 Experimental Results and Estimation of Slenderness Ratio

Tables 2 and 3 provide a summary of the experimental results for circular and square adopted specimens in this study, respectively. Various heights with small increments were tested for each group to specify critical height of CFMST. When CFMST had height less than the critical height, CFMST was behaved as short column (non-slender) and it was behaved as long column (slender) when CFMST’s height exceed the critical height. The value of height increments was 50 mm, as shown by the height of column in Tables 2 and 3. Discussion of the results is in three parts: failure mode, estimation of slenderness ratio, and ultimate strength.

#### 3.1 Failure Mode

Two types of failure mode were observed during the test program (local buckling and global buckling) failure, as shown in Fig. 5. These modes of failure were used to classify columns into slender or non-slender. When local buckling failure occurs, the column behaves as a non-slender column

Table 2 Adopted column specimens with circular section

Group of specimens	Specimen designation	Height of column (mm)	$P_{ultimate}$ (kN)	Mode of failure
C1S	C1S450	450	387	Local Buckling
	C1S500	500	361	Global Buckling
	C1S550	550	328	Global Buckling
	C1S600	600	278	Global Buckling
	C1S650	650	275	Global Buckling
	C1S700	700	259	Global Buckling
	C2S	C2S500	500	471
C2S550		550	446	Global Buckling
C2S650		650	435	Global Buckling
C2S700		700	383	Global Buckling
C2S750		750	376	Global Buckling
C3S	C3S500	500	489	Local Buckling
	C3S550	550	487	Local Buckling
	C3S600	600	484	Global Buckling
	C3S650	650	451	Global Buckling
	C3S700	700	441	Global Buckling
	C3S750	750	386	Global Buckling
	C3S800	800	366	Global Buckling
C2H	C2H400	400	458	Local Buckling
	C2H450	450	380	Local Buckling
	C2H500	500	366	Global Buckling
	C2H550	550	331	Global Buckling
C2H	C2H600	600	255	Global Buckling
	C3H	C3H500	500	446
C3H550		550	401	Local Buckling
C3H600		600	399	Global Buckling
C3H650		650	387	Global Buckling
C3H700		700	340	Global Buckling

**Table 3** Adopted column specimens with square section

Group of specimens	Specimen designation	Height of column (mm)	$P$ ultimate (kN)	Mode of failure
S1S	S1S800	800	380	Local Buckling
	S1S850	850	362	Local Buckling
	S1S900	900	340	Local Buckling
	S1S950	950	338	Local Buckling
	S1S1000	1000	310	Global Buckling
	S1S1100	1100	304	Global Buckling
S2S	S2S800	800	448	Local Buckling
	S2S850	850	393	Local Buckling
	S2S900	900	385	Local Buckling
	S2S950	950	386	Local Buckling
	S2S1000	1000	360	Local Buckling
	S2S1100	1100	320	Global Buckling
S3S	S3S1000	1000	428	Local Buckling
	S3S1050	1050	416	Local Buckling
	S3S1100	1100	382	Local Buckling
	S3S1150	1150	379	Global Buckling
	S3S1200	1200	366	Global Buckling
S2H	S2H700	700	331	Local Buckling
	S2H750	750	292	Local Buckling
	S2H800	800	275	Local Buckling
	S2H850	850	283	Global Buckling
	S2H900	900	231	Global Buckling
S3H	S3H900	900	407	Local Buckling
	S3H950	950	398	Local Buckling
	S3H1000	1000	398	Local Buckling
	S3H1050	1050	385	Local Buckling
	S3H1100	1100	370	Global Buckling

(i.e., short column), and when global buckling failure occurs, column behaves as slender column (i.e., long column). In CFMST columns, the main reason for local and global buckling failures can be justified as follows: when both materials (concrete and steel tubes) reach the yield stress for ductile materials (yielding in steel tube) and the ultimate stress for brittle materials (compressive strength in concrete) at a specific zone in the column, local buckling happened. Global buckling refers to the loss of stability of a component and is usually independent of material strength. This loss of stability usually occurs within the elastic range of the material [32]. Slender or thin-walled components under compressive stress are susceptible to global buckling. Most people have

observed what is called “Euler buckling” where a long slender member subject to a compressive force moves lateral to the direction of that force. Although Euler’s theory of columns applied for isotropic and homogenous materials, but in general, the force necessary to cause such a buckling motion. Therefore, buckling studies are much more sensitive to the component restraints than in a normal stress analysis [33]. The theoretical Euler solution will lead to infinite forces in very short columns, and that clearly exceeds the allowed material stress. Thus, in practice, Euler column buckling can only be applied in certain regions and empirical transition equations are required for intermediate length columns. For very long columns, the loss of stiffness occurs at stresses far below the material failure [34].

Form the failure mode of experimental results shown in Tables 2 and 3, it observed that maximum height of specimen that failed by local buckling increased when use more than one steel layer. For CSMST with circular cross section, it failed by local buckling when maximum height was (450, 500 and 550) mm for C1S, C2S and C3S, respectively, and for CFMST with square section, the maximum height was (1000, 1100 and 1150) mm for S1S, S2S and S3S, respectively. These results led to conclude that the increase number of steel tube eliminated the early global buckling and led the failure mode of specimens to be local buckling rather than global buckling due to increasing stiffness of section.

### 3.2 Estimation of Slenderness Ratio

The main objective of this study and tables is to determine the slenderness ratio for this type of column. The slenderness ratio is the limit between short columns and long columns. In this study, the term “slenderness limit” refers to the limit that is used to specify whether the column is slender or non-slender. This limit is determined when the mode failure of two specimens changes from local to global buckling. In this investigation, Eqs. 1 and 2 were proposed to estimate the slenderness limit for CFMST with various parameters such as type of section (square or circular), number of steel layers, and solid or hollow section.

$$\lambda = \frac{A_S}{A_C} \quad (1)$$

$$S_L = \lambda \cdot h_{av} \quad (2)$$

where

$\lambda$  = represents suggested slenderness ratio, dimensionless.

$A_S$  = Area of steel in cross section of the specimen, mm<sup>2</sup>.

$A_C$  = Area of concrete in cross section of the specimen, mm<sup>2</sup>.

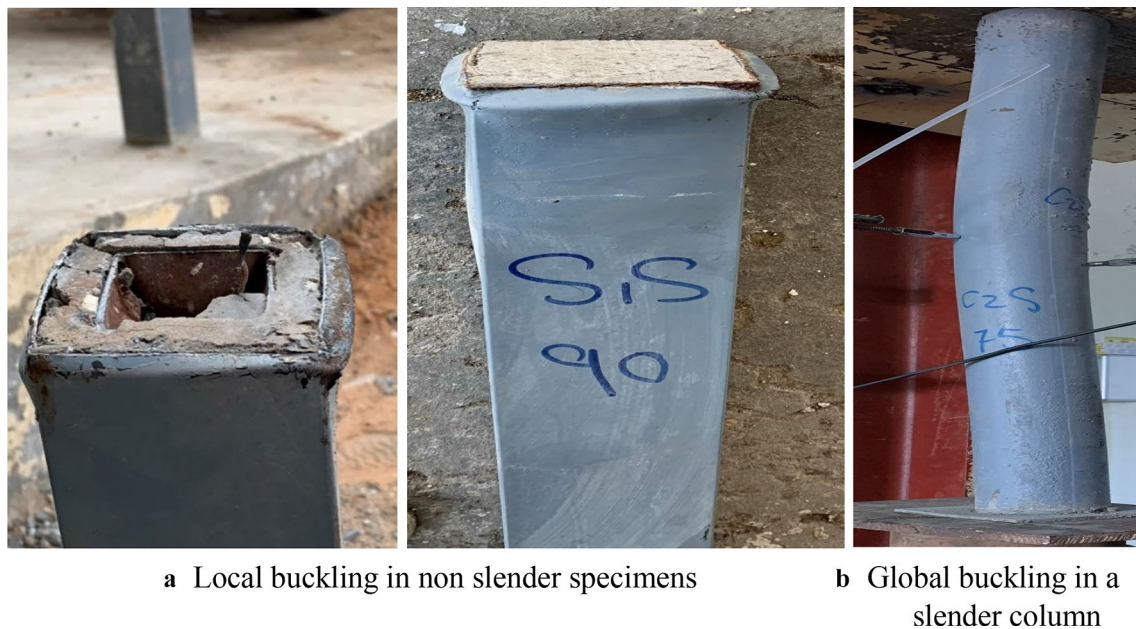


Fig. 5 Observed mode failure in adopted CFMST

$S_L$  = represent slenderness limit for the adopted column, mm.

$h_{av}$  = represents the average height of adjacent specimens when mode failure converted to represent with "local to global buckling", mm.

The slenderness limit of CFMST was calculated for the experimental result depending on suggested Eqs. 1 and 2 as shown in Tables 4 and 5. In Tables 4 and 5, two contiguous columns were chosen for each group, one of which failed by local buckling and one of which failed by global buckling. The point at which the failure type changes from local buckling to global buckling determines the slenderness ratio for each group. From these results, it was observed that the slenderness limit for solid sections

increased with the increased number of steel tubes from (26.12 to 66.12) mm and (53.62 to 129.4) mm for circular and square section, respectively. In the hollow section, the slenderness limit decreased with the increased number of steel tubes in the circular section from (81.22 to 74.75) mm and in the square section from (139.75 to 132.5) mm. This is due to the increased area of the hollow section in relation to the total cross-section area, where the ratio of hollow area to total cross-section area in (C2H and S2H) is equal to (41%) while in (C3H and S3H) it is equal to (9.4%), review Fig. 3. For this reason, the slenderness limit in the hollow section decreases. Another reason for the decrease in the slenderness limit in the hollow section is due the decrease in the concrete area within the cross section of CFMST which affects the proposed equations.

Table 4 Predicted slenderness limit ( $S_L$ ) for adopted CFST with circular section

Group of specimens	Specimen designation	Mode failure	$h_{cr}$ (mm)	$A_s$ (mm <sup>2</sup> )	$A_c$ (mm <sup>2</sup> )	$\lambda$	$S_L$ (mm)
C1S	C1S450	Local	475	236.25	4324.12	0.055	26.12
	C1S500	Buckling					
C2S	C2S500	Local	525	392.7	4167.7	0.094	49.35
	C2S550	Buckling					
C3S	C3S550	Local	575	469.35	4091.02	0.115	66.12
	C3S600	Buckling					
C2H	C2H450	Local	475	392.7	2297.3	0.171	81.22
	C2H500	Buckling					
C3H	C3H550	Local	575	469.35	3660.96	0.13	74.75
	C3H600	Buckling					

**Table 5** Predicted slenderness limit ( $S_L$ ) for adopted CFST with square section

Group of specimens	Specimen designation	Mode failure	$h_{cr}$ (mm)	$A_s$ (mm <sup>2</sup> )	$A_c$ (mm <sup>2</sup> )	$\lambda$	$S_L$ (mm)
S1S	S1S950	Local	975	300.8	5505.64	0.055	53.62
	S1S1000	Buckling					
S2S	S2S1000	Local	1050	500	5306.44	0.094	98.7
	S2S1100	Buckling					
S3S	S3S1100	Local	1125	597.6	5208.8	0.115	129.4
	S3S1150	Buckling					
S2H	S2H800	Local	825	500	2925	0.171	132.5
	S2H850	Buckling					
S3H	S3H1050	Local	1075	597.6	4661.28	0.13	139.75
	S3H1100	Buckling					

It was also observed that the slenderness limit of the square section was approximately twice the slenderness limit for the circular section, because the area of the circular section is less than the area of the square section for the same external dimension by 22.5%.

### 3.3 Ultimate Strength

The ultimate strength and the load–lateral displacement relationship of the adopted specimens was shown in Figs. 6 and 7 for CFMST column with circular and square, respectively. It observed that use more than one steel layer increased the ultimate strength of section. While the used of hollow section instead of full filled steel tube section reduced the ultimate strength. This is due to increase the concrete in cross section. Some parametric studies were adopted from results shown in Table 6 and 7 as follows.

For specimens with the same column height, Tables 6 and 7 explain a comparison study for ultimate strength of the adopted CFMST for circular and square section, respectively. The study showed that the ultimate strength of CFMST increases with an increased number of steel tubes by a ratio of (70.3–30.5) % for circular section and (38.1–5.3) % for square section over the ultimate strength of CFST column with a single steel layer, depending on the height and number of steel tubes. In circular section, experimental results indicated that in circular section the ratio increased as column height increased, while in square section it was the reverse. The structural behavior of CFST elements is considerably affected by the difference between the Poisson 's ratios of the steel tube and concrete core. In the initial stage of loading, the Poisson's ratio for the concrete is lower than that of steel. Thus, the steel tube has no confining effect on the concrete core. As longitudinal strain increases, the lateral expansion of the concrete gradually becomes greater than the expansion of the steel tube. At this stage, the concrete core becomes triaxially and steel tube biaxially stressed [33]. The steel tube under a biaxial state cannot sustain the normal

yield stress, causing a transfer of load from tube to the core. The load transfer mechanism is similar in square and circular CFST elements. In the first stage of loading, the steel tube sustains most of the load until it yields.

Even though the load transfer mechanism in circular and square CFST is similar, the maximum confined compressive stress of concrete core in circular columns is higher than in square column. This can be explained in terms of a larger confining effect of circular steel tubes.

## 4 Conclusions

Based on the results achieved from the experimental work, the main conclusions can be drawn as:

1. A new suggested equation was used to calculated the slenderness limit of CFST with the various numbers of steel tubes which leads to knowing the column behave as slender or non-slender.
2. It was observed that the slenderness limit of CFST increased with an increased number of steel layers (skins). For the solid section, it increased from (26.12 to 66.12) mm for the circular section and (53.62 to 129.4) mm for the square section.
3. In the hollow section of CFST, it was observed that the slenderness limit decreased with the increased number of steel skins from (81.22 to 74.75) mm for the circular section and (132.5 to 139.75) mm for square section. This is due to the increased hollow ratio of the sectional area in relation to the total cross-section area.
4. The slenderness limit of the square section is more twice the value of that of the circular section. This is due to the area of the circular section being ( $\pi/4 = 22.5\%$ ) less





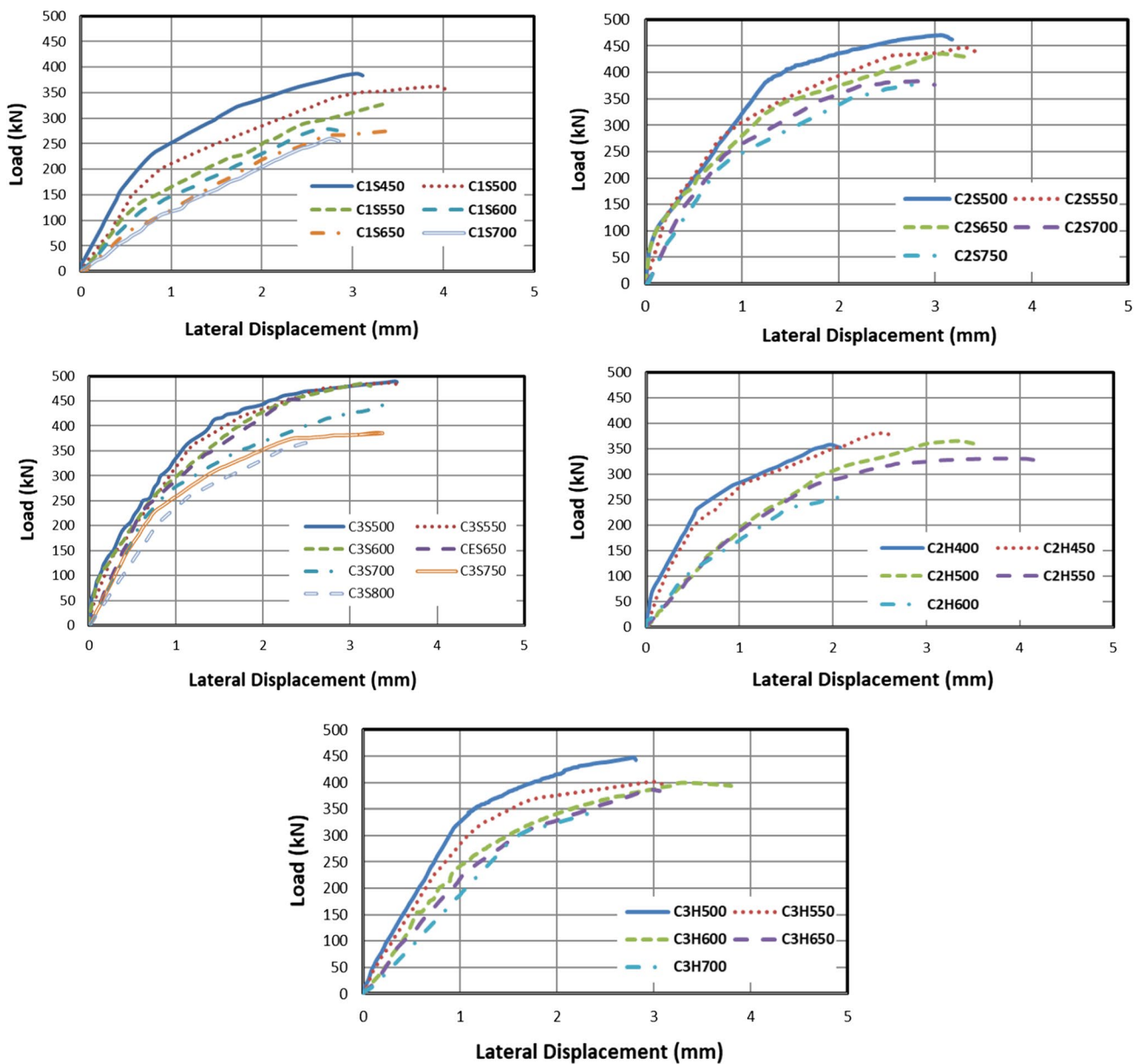


Fig. 6 Load-lateral displacement relation for CFMST with circular section

than the area of the square section for the same external dimension.

5. The ultimate strength of CFMST column increases with increased numbers of steel layers by a ratio of (70.3–

30.5) % for circular section and (38.1–5.3) % for square section over the ultimate strength of CFST column with a single steel layer.

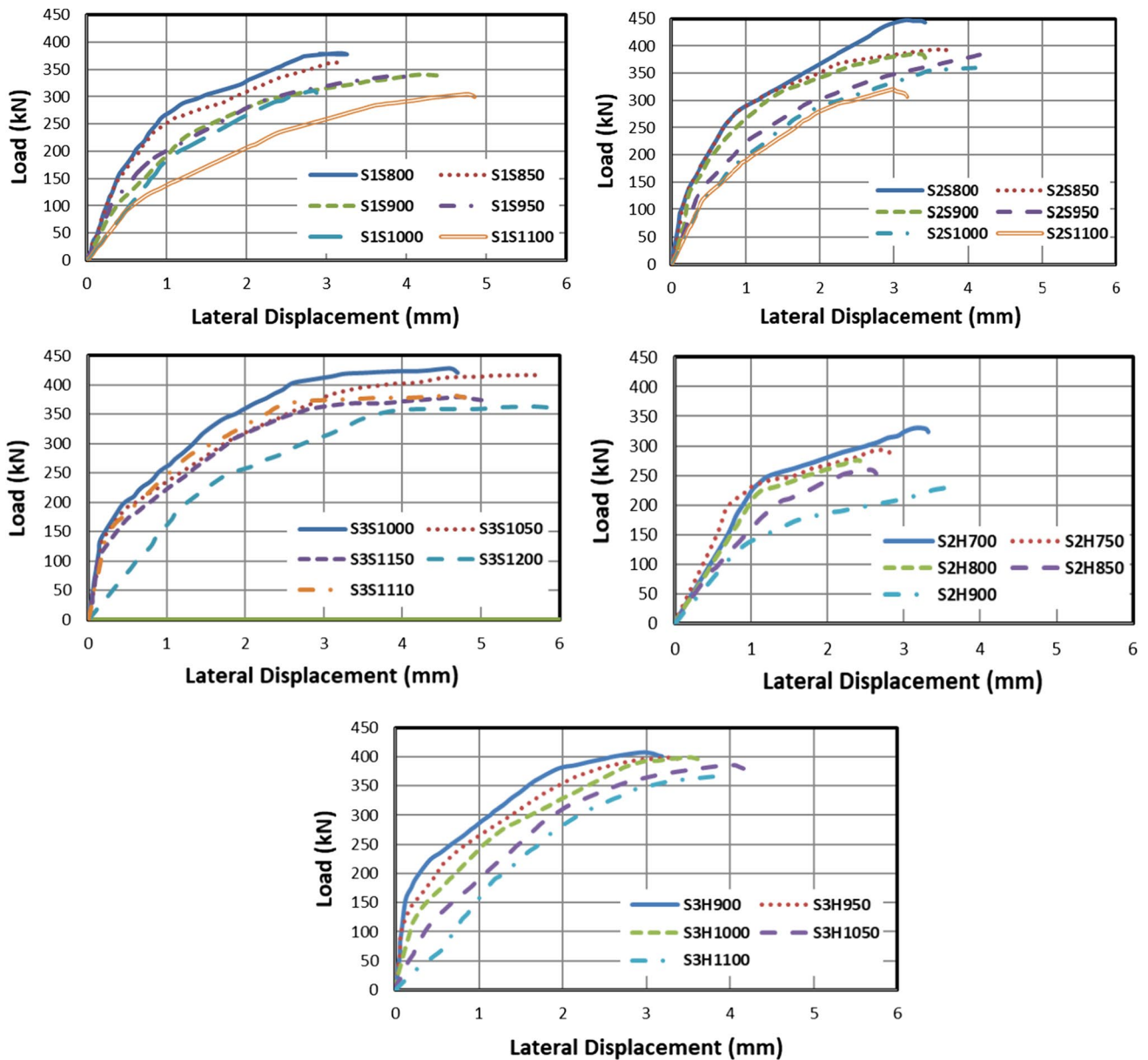


Fig. 7 Load-lateral displacement relation for CFMST with square section

Table 6 Comparison study for ultimate strength for circular section

Height of column (mm)	P ultimate (kN)			Increase ratio (%) <sup>a</sup>	
	C1S	C2S	C3S	C2S	C3S
500	361	471	489	30.5	35.5
550	328	446	487	35.6	48.5
650	275	435	451	58.2	64.0
700	259	383	441	47.9	70.3

<sup>a</sup>Increase ratio (%) =  $\frac{CNS-CIS}{CIS} \times 100$

Table 7 Comparison study for ultimate strength for square section

Height of column (mm)	P ultimate (kN)			Increase ratio (%) <sup>a</sup>	
	S1S	S2S	S3S	S2S	S3S
1000	310	360	428	16.1	38.1
1100	304	320	382	5.3	25.7

<sup>a</sup>Increase ratio (%) =  $\frac{SNS-S1S}{S1S} \times 100$

## References

- Ekmeçyapar, T.; Hasan, H.G.: The influence of the inner steel tube on the compression behaviour of the concrete filled double skin steel tube (CFDST) columns. *Mar. Struct.* **66**(2018), 197–212 (2019). <https://doi.org/10.1016/j.marstruc.2019.04.006>
- Lai, H.J.; Hanzic, L.: Fillers to improve passing ability of concrete. *Struct. Concr.* **20**, 185–197 (2019)
- Lai, H.J.; Binhowimal, S.A.M.; Hanzic, L.; Wang, Q.: Cause and mitigation of dilatancy in cement powder paste. *Constr. Build. Mater.* **236**, 117595 (2020)
- Peng, Y.Y.; Tan, K.F.: Mechanical properties of duplex steel tube high-strength concrete short columns under axial compression. *J. Wuhan Univ. Technol.* **33**(2), 105–109 (2011)
- Chang, Z.Y.; Ru, Z.L.; Zhou, W.: Study on concrete-filled stainless steel-carbon steel tubular (CFSCST) stub columns under compression. *Thin-Walled Struct.* **63**, 125–133 (2013)
- Ekmeçyapar, A.-E.B.: Concrete filled double circular steel tube (CFDCST) stub columns. *Eng. Struct.* **135**, 68–80 (2017)
- Xiong, L.J.; Xiong, D.X.: Axial performance of short concrete filled steel tubes with high- and ultra-high-strength materials. *Eng. Struct.* **136**, 494–510 (2017)
- Romero, H.A.; Ibañez, C.; Espinós, A.; Portolés, J.M.: Influence of ultra-high strength concrete on circular concrete-filled dual steel columns. *Structure* **9**, 13–20 (2017)
- Ibañez, A.V.; Romero, M.L.; Espinós, A.; Portolés, J.M.: Ultra-high strength concrete on eccentrically loaded slender circular concrete-filled dual steel columns. *Structure* **12**, 64–74 (2017)
- Xiong, L.J.; Xiong, D.X.: Behaviour of steel tubular members infilled with ultra high strength concrete. *J. Constr. Steel Res.* **138**, 168–183 (2017)
- Ahmed, H.M.; Liang, Q.Q.; Patel, V.I.: Behavior of eccentrically loaded double circular steel tubular short columns filled with concrete. *Eng. Struct.* **201**, 109790 (2019)
- Hastemoglu, H.; Erkan, I.: Behaviour of double skinned composite columns with concrete filled tubular columns. *J. Archit. Eng. Technol.* (2017). <https://doi.org/10.4172/2168-9717.1000194>
- Al-Khekany, A.M.; Al-Yassri, L.S.; Abbas, H.S.: An experimental investigation of hollow composite column reinforced by multi-skin square and round steel tube. *Int. J. Civ. Eng. Technol.* **9**(11), 784–793 (2018)
- EN 1994-1-1 (English): Eurocode 4: Design of composite steel and concrete structures – Part 1-1: General rules and rules for buildings [Authority: The European Union Per Regulation 305/2011, Directive 98/34/EC, Directive 2004/18/EC] (2004)
- Balasubramani, N.; Thenmozhi, R.: Strength and deflection of axially loaded DSHCFT columnshaving PVC inner—steel outer pipes annually in-filled with SCC M35. *Indian J. Sci. Technol.* **8**(April), 11–15 (2015). <https://doi.org/10.17485/ijst/2015/v8iS7/62242>
- Ostrowski, K.; Dudek, M.; Sadowski, Ł.: Compressive behaviour of concrete-filled carbon fiber-reinforced polymer steel composite tube columns made of high performance concrete. *Compos. Struct.* **234**, 111668 (2020). <https://doi.org/10.1016/j.compstruct.2019.111668>
- Alwash, N.A.; Al-Salih, H.I.: Experimental investigation on behavior of SCC filled steel tubular stub columns strengthened with CFRP. *Constr. Eng.* **1**(2), 37–51 (2013)
- Zeghiche, J.; Chaoui, K.: An experimental behaviour of concrete-filled steel tubular columns. *J. Constr. Steel Res.* **61**(1), 53–66 (2005). <https://doi.org/10.1016/j.jcsr.2004.06.006>
- Furlong, R.W.: Strength of steel-encased concrete beam columns. *J. Struct. Div. ASCE* **93**(5), 113–124 (1967)
- Knowles, P.R.: Strength of concrete filled steel columns. *J. Struct. Div., ASCE* **95**(12), 2565–2587 (1969)
- Neogi, C.J.; Sen, H.: Concrete-filled tubular steel columns under eccentric loading. *Struct. Eng.* **47**(5), 187–195 (1969)
- Rangan, J.M.: Strength of eccentrically loaded slender steel tubular columns filled with high-strength concrete. *ACI Struct. J.* **89**(6), 676–681 (1992)
- Zeghiche, C.K.: An experimental behaviour of concrete-filled steel tubular columns. *J. Constr. Steel Res.* **61**(1), 53–66 (2005)
- Portolés, F.F.; Romero, M.L.; Bonet, J.L.: Experimental study of high strength concrete-filled circular tubular columns under eccentric loading. *J. Constr. Steel Res.* **67**(4), 623–633 (2011)
- Dundu, M.: Compressive strength of circular concrete filled steel tube columns. *Thin-Walled Struct.* **56**, 62–70 (2012)
- Ekmeçyapar, A.-E.B.: Experimental behaviour of circular concrete filled steel tube columns and design specifications. *Thin-Walled Struct.* **105**, 220–230 (2016)
- Tao, Z.X.; Han, L.H.: Behaviour of concrete-filled double skin (CHS inner and CHS outer) steel tubular stub columns and beam-columns. *J. Constr. Steel Res.* **60**(8), 1129–1158 (2004)
- Romero, I.C.; Espinós, A.; Portolés, J.M.; Hospitaler, A.: Slender double-tube ultra-high strength concrete-filled tubular columns under ambient temperature and fire. *Eng. Struct.* **99**, 536–545 (2015)
- Wan, Z.X.: Nonlinear analysis and design of concrete-filled dual steel tubular columns under axial loading. *Steel Comp. Struct.* **20**(3), 571–597 (2016)
- Ahmed, M.; Liang, Q.Q.; Patel, V.I.; Hadi, M.N.S.: Computational simulation of eccentrically loaded circular thin-walled concrete-filled double steel tubular slender columns. *Eng. Struct.* **213**(2019), 110571 (2020). <https://doi.org/10.1016/j.engstruct.2020.110571>
- Dixon, D.E.; et al.: Standard Practice for Selecting Proportions for Normal, Heavyweight, and Mass Concrete (ACI 211.1-91) (1991)
- Ziegler, H.: Principles of Structural Stability. Gill-Blaisdell, Waltham (1968)
- Kuranovas, A.; Kvedaras, A.K.: Behaviour of hollow-concrete steel tubular composite elements. *J. Civ. Eng. Manag.* **13**(2), 131–141 (2007)
- Young, W.G.; Budynas, R.G.: Roark's Formulas for Stress and Strain, 7th edn. Mc Graw-Hill, New York (2002)

